scientific reports

Check for updates

OPEN

Leukemia cells remodel bone marrow stromal cells to generate a protumoral microenvironment via the S100A8-NOX2-ROS signaling pathway

Yangyang Gu[1,3,5], Jingyi Xia[2,5], Yuhong Guo[1,3], Linfen Tao[1,3], Guanbin Zhang[1,3,4]✉ & Jianping Xu[1,3]✉

The bone marrow microenvironment (BMM) plays a crucial role in the pathogenesis and progression of acute myeloid leukemia (AML). AML cells can modify the BMM to establish a more favorable environment for their survival. However, the mechanism about the complex regulatory interplay between the BMM and AML cells remains unclear. In this study, we used proteomic analysis to elucidate the potential mechanisms underlying the interaction between bone marrow stromal cells (BMSCs) and AML cells. We found that the co-culture of AML cells and BMSCs facilitated the proliferation of AML cells, suppressed the proliferation of BMSCs and triggered their senescence. Furthermore, we show the aberrant expression of S100A8 that plays a crucial role in the communication between AML cells and BMSCs. In the co-culture system, overexpression of S100A8 in AML cells activated NOX2 and induced the production of reactive oxygen species (ROS) in the supernatant, thereby suppressing the proliferation of BMSCs and facilitating the senescence of BMSCs. Subsequently, aging BMSCs secreted a variety of cytokines, including IL-6, CXCL5, MIP-1b, etc. as shown by Cytokine Array and qPCR analysis, which had stimulatory effects on the progression of AML. In conclusion, the present study reveals the crucial involvement of the S100A8-NOX2-ROS signaling pathway in mediating communication between AML cells and BMSCs, suggesting that targeting S100A8 may constitute an efficient strategy for AML therapy.

Keywords Acute myeloid leukemia, Bone marrow microenvironment, Bone marrow stromal cells, S100A8-NOX2-ROS signaling pathway, Cytokines

Acute myeloid leukemia (AML) is a hematological malignancy characterized by the abnormal proliferation and differentiation of hematopoietic cell precursors in the bone marrow, disrupting normal hematopoiesis and causing bone marrow failure[1]. AML is the most common type of acute leukemia in adults, with a low rate of remission and a tendency to relapse[2]. Chemotherapy is the main treatment for AML, with a cure rate of 35–40% in adult patients below 60 years of age and merely 5–15% in those over 60[1]. The bone marrow microenvironment (BMM) plays a crucial role in the pathogenesis and progression of AML, serving as the direct niche for leukemia cells[3,4]. The BMM is composed of stromal cells, extracellular matrix, cytokines and other constituents that provide direct or indirect support to leukemia cells, thereby enabling them to acquire a static stem cell phenotype, and shielding them from both spontaneous and therapeutic apoptosis[3,5,6]. At the same time, leukemia cells can modify the BMM to establish an even more favorable environment for their survival[7,8]. Investigating the complex regulatory interplay between the BMM and AML cells is essential to understanding the development of leukemia and achieving a cure.

[1]Department of Laboratory Medicine, School of Medical Technology and Engineering, Fujian Medical University, Fuzhou, Fujian, China. [2]Department of Blood Transfusion, Fujian Medical University Union Hospital, Fuzhou, Fujian, China. [3]Key Laboratory of Clinical Laboratory Technology for Precision Medicine (Fujian Medical University), Fujian Province University, Fuzhou, Fujian, China. [4]School of Intelligent Medicine, Chengdu University of Traditional Chinese Medicine, Chengdu, Sichuan, China. [5]Yangyang Gu and Jingyi Xia contributed equally to this work. ✉email: gbzhang@capitalbio.com; jianpingxu@fjmu.edu.cn

S100A8 is a calcium- and zinc-binding protein with diverse intracellular and extracellular functions[9,10]. Aberrant expression of S100A8 has been observed in several tumors, including hematological malignancies[11,12]. Overexpression of S100A8 can impede the differentiation of AML cells[13]. The NADPH oxidase NOX2 is highly active in AML patients[14,15]. NOX2 can stimulate glycolysis and proliferation of AML cells by activating PFKFB3[16], and NOX2 can facilitate mitochondrial transfer from bone marrow stromal cells (BMSCs) to AML cells by generating reactive oxygen species (ROS), thus providing the energy needed for the rapid proliferation of AML cells[17]. Previous studies have demonstrated that S100A8 can activate NOX2 through direct interaction with NCF2 (a.k.a. $p67^{phox}$), a regulatory subunit of NOX2[14,18]. Furthermore, silencing S100A8 in mouse microglioma cells led to a decrease in the expression of NOX2[19]. This suggests that S100A8 has the ability to modulate the activation and expression of NOX2. However, it remains unclear whether S100A8 can regulate ROS production by activating NOX2 in AML.

ROS, which include superoxide anion, hydrogen peroxide and others, can induce DNA damage and cellular senescence, which also contribute to the remodeling of hematopoiesis and the tumor microenvironment[20,21]. The connection between the development of leukemia and the senescence of BMM has been observed[22,23]. Notably, the BMSCs of AML patients exhibit a distinct senescence phenotype compared to healthy donors; moreover, BMSCs from patients with acute lymphoblastic leukemia (mostly children and adolescents) also display a senescence phenotype[24,25]. These findings suggest that senescence of BMSCs plays an important role in the development of acute leukemia. Furthermore, it has been reported that eliminating senescent BMSCs can significantly increase the survival rate of AML mice[26]. Senescent cells are capable of secreting numerous cytokines, a process known as Senescence-Associated Secretory Phenotype (SASP)[27], which can contribute to the progression of AML by activating several signaling pathways or forming a pro-inflammatory microenvironment[28–30].Cytokines are also important mediators that are involved in communication between AML cells and BMSCs[31]. Cytokine imbalance has been reported in the BMM of AML[31,32], where cytokines bind to receptors and activate cell-surface receptor-regulated signal transduction pathways, and contribute to autocrine or paracrine loops[33,34], increasing the supportive role of the BMM, promoting the progression of AML towards a more malignant phenotype. Therefore, targeting the interaction between leukemia cells and the BMM may represent an effective therapeutic strategy.

Based on the literature and current knowledge, the purpose of this study is to investigate the reciprocal regulatory interaction between AML cells and BMSCs, along with elucidating the underlying molecular mechanisms. Ultimately, this research will provide a strong foundation for the discovery of new targets about the interaction between AML cells and BMSCs.

Results

Analysis of differentially expressed proteins in U937 cells co-cultured with or without HS-5 cells

To investigate the relationship between AML cells and BMSCs, proteomic analysis was initially performed on AML cells before and after co-culture with BMSCs. A total of 938 proteins was found to be differentially expressed in U937 cells after co-culture with HS-5 cells. 489 proteins displayed increased expression ($Fc > 2$ and $p < 0.05$), with 96 proteins exhibiting a $Fc > 10$ and $p < 0.05$, while 449 proteins showed decreased expression ($Fc < 0.5$; $p < 0.05$), including 27 proteins with a $Fc < 0.1$ and $p < 0.05$ (Fig. 1A,B). KEGG enrichment analysis was conducted on the differentially expressed proteins. For upregulated proteins, KEGG terms mainly mapped to pathways involved in transport and catabolism processes, as well as pathways associated with environmental signal transduction. Some examples are the NOD-like receptor signaling pathway, phagosome and IL-17 signaling pathway (Fig. 1C). For the downregulated proteins, KEGG data were mapped to the cell cycle and DNA replication (Fig. 1D).

Co-culture with HS-5 cells inhibits apoptosis and promotes the proliferation of U937 cells

We initially evaluated the impact of co-culture with HS-5 stromal cells on the proliferation and apoptosis of AML cells. When co-cultured with HS-5 cells, U937 cells exhibited a significant increase in viability compared with controls (Fig. 2A). Additionally, the apoptosis rate of U937 cells was significantly decreased after co-culture (Fig. 2B,C). Overall, co-culture of AML cells with BMSCs promoted the proliferation of AML cells while concurrently suppressing their apoptosis.

Co-culture with HS-5 cells promotes ROS production through the activation of NOX2 in U937 cells

Proteomic analysis revealed an up-regulation of the expression of NOX2 in U937 cells co-cultured with HS-5 cells (Supplementary Table S2). Furthermore, NOX2 was found to be associated with the NOD-like receptor signaling pathway as indicated by the KEGG enrichment analysis. This prompted us to investigate whether NOX2 is involved in the reciprocal regulation between AML cells and BMSCs. Western blot analysis illustrated that the protein levels of NOX2 were increased after co-culture with HS-5 cells (Fig. 3A,B). We then assessed NOX2 activity in the supernatant and the intracellular ROS levels of U937 cells co-cultured with or without HS-5 cells. After co-culture with HS-5 cells, NOX2 activity in U937 cells was significantly increased (Fig. 3C). Additionally, the ROS levels in the supernatant were also significantly increased (Fig. 3D), while intracellular ROS levels were significantly reduced (Fig. 3E,F). These results suggested that co-culture of U937 with BMSCs promoted ROS production through activating NOX2 activity in AML cells.

A

Cell line	Fc > 2	Fc < 0.5	Fc > 10	Fc < 0.1
U937(coC VS moC)	489	449	96	27

B

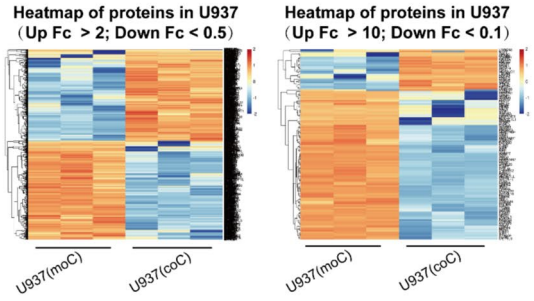

C

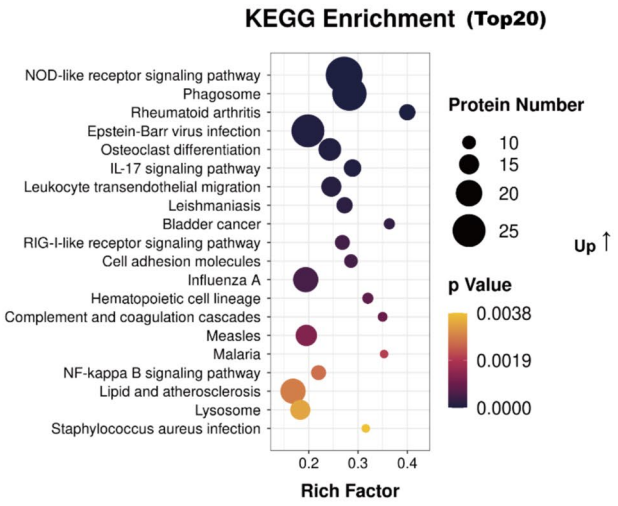

D

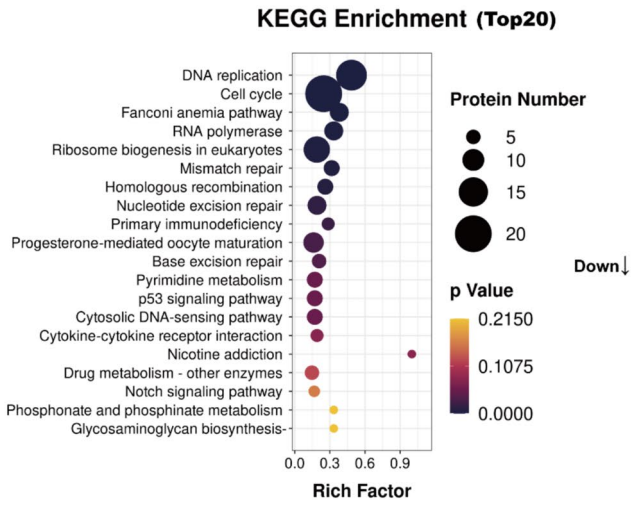

Fig. 1. Analysis of differentially expressed proteins in U937 cells co-cultured with or without HS-5 cells. Proteomic analysis was performed to identify differentially expressed proteins in U937 cells co-cultured with (coC) or without (moC) HS-5 cells. Results are the means of three replicates for each group. (**A**) Number of differentially expressed proteins; (**B**) Heatmap of cluster analysis of differentially expressed proteins in U937 cells co-cultured with or without HS-5 cells. The KEGG pathway enrichment of the upregulated (**C**) and downregulated (**D**) proteins in U937 cells after co-culture is shown. The diameter and the depth of color of the solid circles represent the number of differentially expressed proteins and *p* values, respectively.

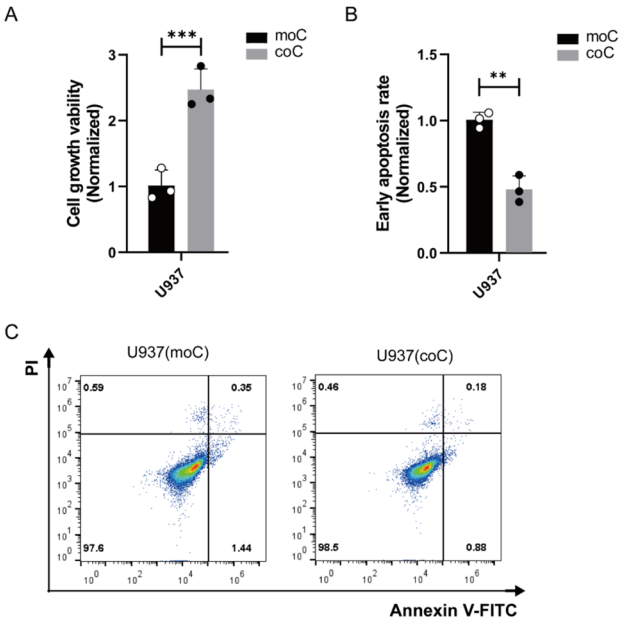

Fig. 2. Changes in the biological activities of U937 cells co-cultured with or without HS-5 cells. The proliferation and apoptosis of U937 cells co-cultured with (coC) or without (moC) HS-5 cells were evaluated. (**A**) Cell viability was assessed using the MTS assay at 48 h, (**C**) Apoptosis was measured by Annexin V-FITC/PI double staining after 48 h and the quantitative analyses are shown in (**B**). The experiments were repeated three times. * $p < 0.05$, ** $p < 0.01$, *** $p < 0.001$.

S100A8 stimulates ROS production via activating NOX2 in U937 cells co-cultured with HS-5 cells

According to the results of the proteomic analysis, the expression of S100A8 is also up-regulated in U937 cells co-cultured with HS-5 cells (Supplementary Fig. 1). Consequently, an intriguing question arises as to whether S100A8 can stimulate ROS production by activating NOX2 in AML cells. Three shRNA sequences targeting S100A8 were designed to construct S100A8-lentiviral shRNA for knocking down this protein in U937 cells, The second sequence showed relatively obvious depletion of S100A8 protein levels (Supplementary Fig. 2). Western blot analysis showed that the protein level of NOX2 was decreased after S100A8 knockdown (Fig. 3G,H). Meanwhile, S100A8 knockdown significantly attenuated NOX2 activity and extracellular ROS levels in U937 cells co-cultured with HS-5 cells (Fig. 3I,J) while increasing intracellular ROS levels (Fig. 3K,L). Taken together, these results demonstrated that S100A8 could regulate ROS production by activating NOX2 in AML cells co-cultured with BMSCs.

HS-5 cells co-cultured with U937 cells demonstrate senescence

Co-culture of U937 cells and BMSCs can result in an elevation of extracellular ROS, prompting further investigation whether co-culture can induce a senescent phenotype in BMSCs. Our studies showed that co-culture with U937 cells could inhibit the proliferation of HS-5 cells (Fig. 4A,B). Additionally, we also found that co-culture with U937 cells could induce senescence in HS-5 cells (Fig. 4E,F). Given the observed reduction in ROS levels in the supernatant upon knockdown of S100A8 in U937 cells, we examined the effects of S100A8-KD in U937 cells on the cell viability and senescence phenotype of HS-5 cells. Our study demonstrated that S100A8 knockdown in U937 cells could lead to an increase in the cell viability and inhibition of senescence of HS-5 cells (Fig. 4C,D Fig. 4G,H). These results showed that S100A8 played a crucial role in the senescence of BMSCs when co-cultured with U937 cells.

Changes of cytokines in the supernatant of U937 cells co-cultured with or without HS-5 cells

HS-5 cells exhibited a senescence phenotype after co-culture with U937 cells, prompting us to investigate potential changes in the expression levels of SASP. A Cytokine Array was used to analyze the cytokine production in the supernatant of U937 cells co-cultured with or without HS-5 cells. We observed elevated levels of multiple cytokines in the co-culture supernatants, with chemokines exhibiting the highest variability. Knockdown of S100A8 expression in U937 cells resulted in reduced levels of various cytokines including IL-6, CXCL5, GM-CSF, MIP-1β, etc. in the supernatants of co-cultures (Fig. 5A-C, Supplementary Table S3, Supplementary Fig. 9). Besides, we further verified the expression of related cytokines by RT-qPCR assay, which was consistent with the results of Cytokine Array (Fig. 5D-E). Collectively, this indicates that S100A8 modulates cytokine production and might serve as a crucial target to regulate the interaction between AML cells and BMSCs.

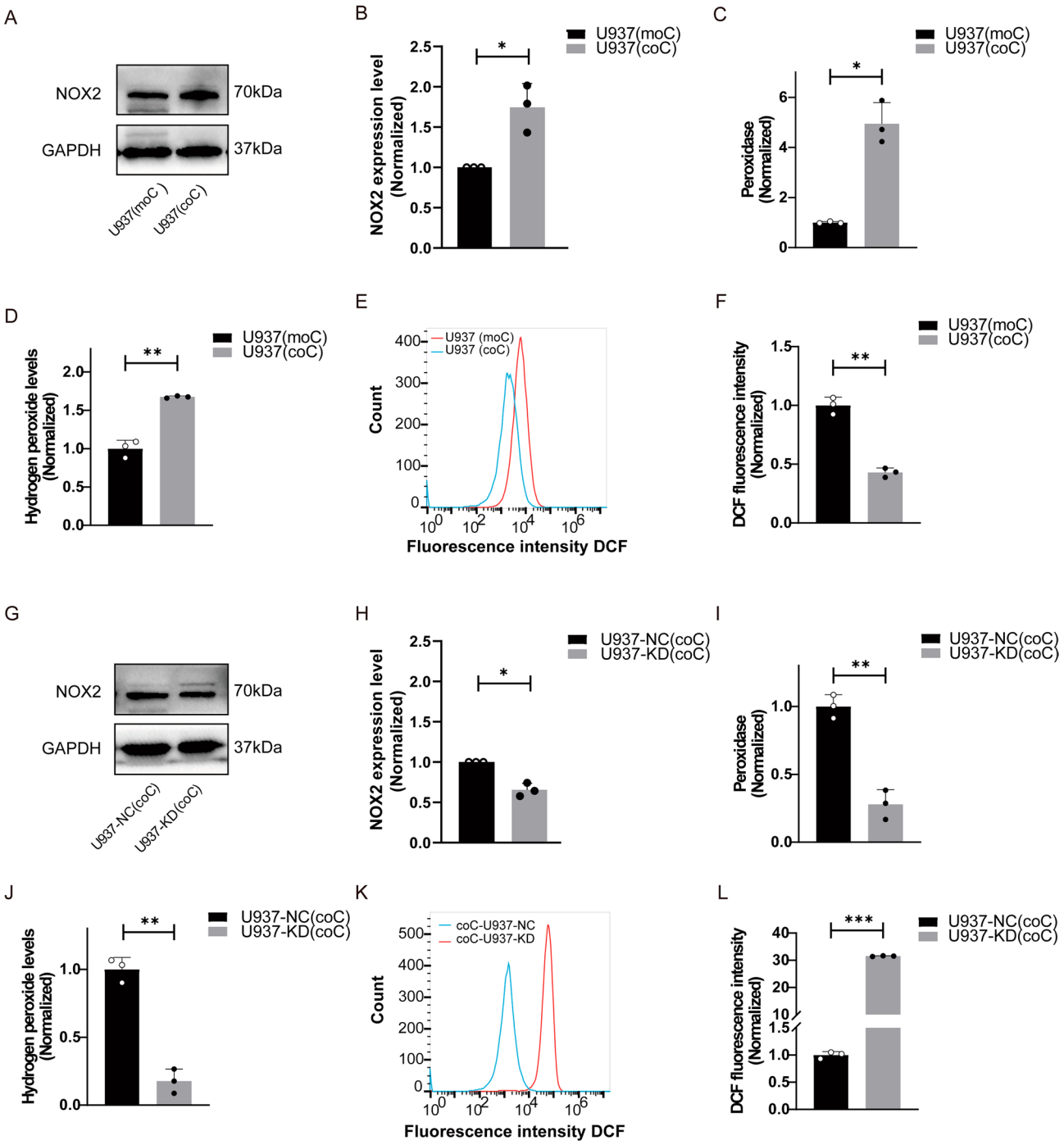

Fig. 3. Enzymatic activity of NOX2 and extracellular and intracellular ROS levels in U937 cells co-cultured with or without HS-5 cells. The protein levels of NOX2 were determined via Western blot in U937 cells co-cultured with or without HS-5 cells (**A**) and were quantified and normalized to GADPH (**B**); The enzymatic activity of NOX2 (**C**) and the levels of ROS in the supernatant (**D**) in U937 cells co-cultured with HS-5 cells (coC) at 48 h were detected by the Amplex red assay. The intracellular ROS levels of U937 cells at 48 h were detected by the DCFH-DA probe (**E**). The quantitative analyses are shown in (**F**); The protein levels of NOX2 were determined via Western blot in U937 cells or S100A8-KD U937 cells (U937-KD) co-cultured with HS-5 cells (**G**) and were quantified and normalized to GADPH (**H**);The enzymatic activity of NOX2 (**I**) and the levels of ROS in the supernatant (**J**) in S100A8-KD U937 cells (U937-KD) co-cultured with HS-5 cells at 48 h were detected by the Amplex red assay. The intracellular ROS levels of the S100A8-KD U937 cells (U937-KD) at 48 h were detected by DCF probe (**K**). The quantitative analyses results are shown in **L**. The experiments were repeated three times. * $p < 0.05$, ** $p < 0.01$, *** $p < 0.001$.

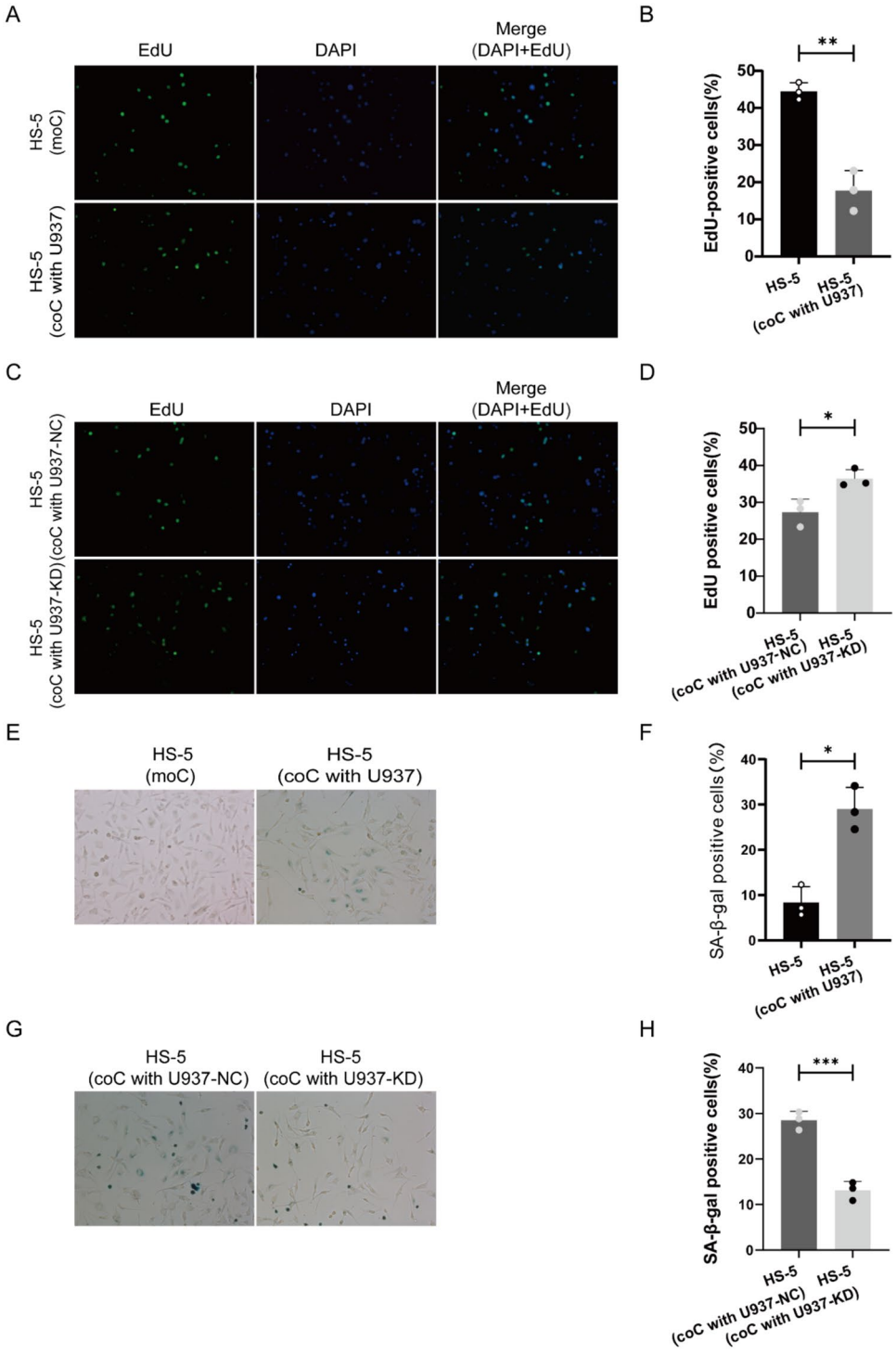

Fig. 4. Results of EdU staining and SA-β-Gal staining of HS-5 cells co-cultured with or without U937 and S100A8-KD U937 cells. After co-culture with U937 cells for 48 h, staining for EdU was determined in HS-5 cells, and images were observed using 200X fluorescence microscopy after staining the nuclei of proliferating cells with EdU (green) and the nuclei of all cells with DAPI (blue) (**A**); After co-culture with U937 or S100A8-KD U937 cells (U937-KD) for 48 h, HS-5 cells were examined after staining EdU (**C**); The proportion of EdU positive cells was calculated by the ratio of EdU positive cells to the number of DAPI positive nuclei. The quantitative analyses are shown in (**B & D**). After co-culture with U937 cells for 48 h, staining for SA-β-Gal was determined in HS-5 cells. (**E**) Representative images of SA-β-Gal signal were captured using a fluorescence microscope fitted with a 20X objective; (**F**) The percentage of SA-β-Gal$^+$ cells in each group was assessed; Staining for SA-β-Gal was also determined in HS-5 cells after co-culture with U937 or S100A8-KD U937 cells (U937-KD) for 48 h. Representative images were captured as in (**G**); (**H**) The percentage of SA-β-Gal$^+$ cells in each group was calculated. The experiments were repeated three times. * $p < 0.05$, ** $p < 0.01$.

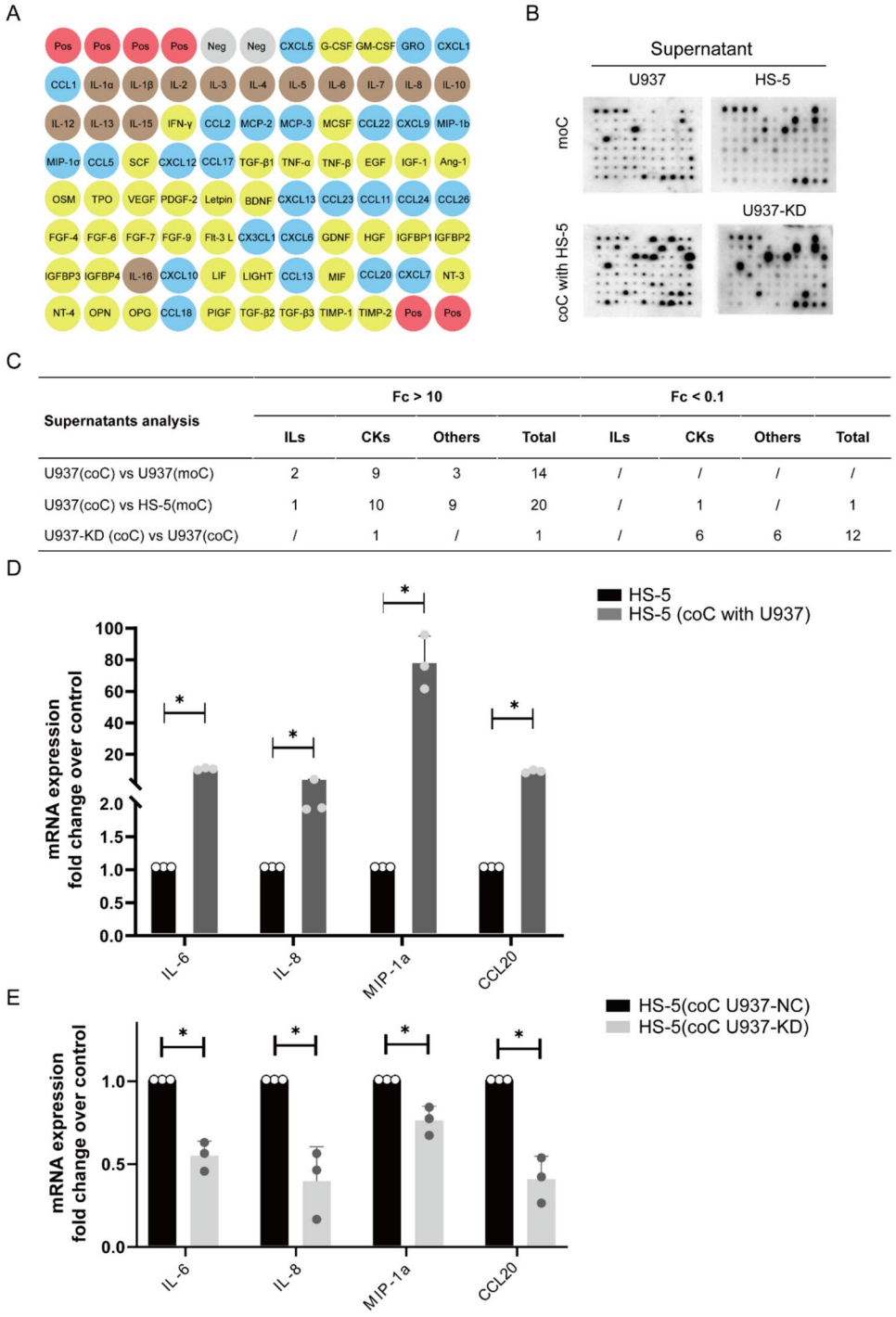

Supernatants analysis	Fc > 10				Fc < 0.1			
	ILs	CKs	Others	Total	ILs	CKs	Others	Total
U937(coC) vs U937(moC)	2	9	3	14	/	/	/	/
U937(coC) vs HS-5(moC)	1	10	9	20	/	1	/	1
U937-KD (coC) vs U937(coC)	/	1	/	1	/	6	6	12

Fig. 5. Alteration of the cytokine production in the supernatants of co-cultures and mRNA expression of intracellular cytokines in HS-5 cells co-cultured with or without U937 and S100A8-KD U937 cells. (**A**) The supernatants from U937, HS-5, and U937 cells co-cultured with HS-5 cells, as well as S100A8-KD U937 cells (U937-KD) cells co-cultured with HS-5 cells were obtained at 48 h, and were subjected to cytokine array analysis; The results were photographed and presented in (**B**). The grayscale values for each cytokine on the array were obtained using Image J, and subsequently subtracted from the average grayscale values of the two negative controls (minus background). The average grayscale values of six positive control points of the HS-5 supernatant served as standard. The differential expression levels of cytokines between different groups were analyzed based on Fc > 10 and Fc < 0.1 (**C**). Pos, positive control, Neg, negative control, ILs, interleukins, CKs, chemokines. RT-qPCR was conducted to measure the mRNA levels of cytokines IL-6, IL-8, MIP-1a, MIP-3a, with GAPDH as the internal reference gene for quantitative analysis (**D**-**E**). The experiments were repeated triple times. * $p < 0.05$, ** $p < 0.01$, ** $p < 0.001$.

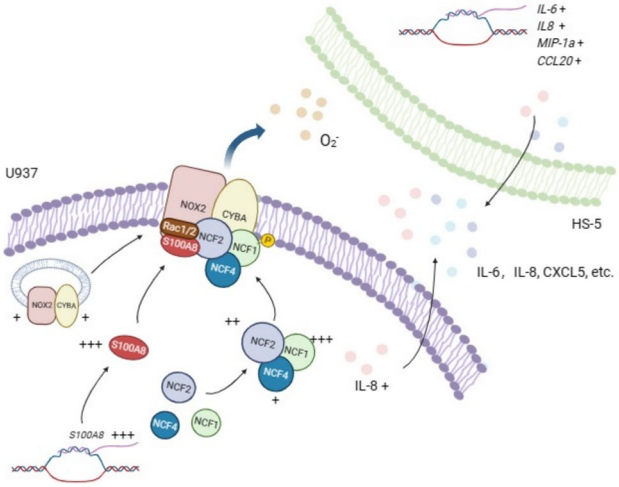

Fig. 6. The potential mechanisms of reciprocal regulation between AML cells and BMSCs. NOX2 and CYBA form heterodimers, which subsequently assemble into the NOX2-CYBA complex in its resting state. Upon activation by intracellular regulatory subunits (NCF1, NCF2, NCF4, etc.), the quiescent NOX2-CYBA complex undergoes electron transfer within NOX2 to generate superoxide anions that are further converted into ROS. Aberrant expression of S100A8 in AML cells can induce the generation of ROS via NOX2 activation, thereby promoting senescence of BMSCs. Aging BMSCs can secrete a variety of cytokines that exert stimulatory effects on the progression of AML. The activation process of NOX2 and the process of cytokine secretion are illustrated. The blue thick arrows indicate extracellular superoxide production.

Discussion

The BMM serves as a crucial niche for the survival of AML cells[3]. Previous studies have demonstrated that BMSCs play a pivotal role in promoting the malignant biological behavior of AML cells [6,35]. In addition to U937 cells, we successfully replicated the previous findings in another AML cell line, HL-60 cells, as anticipated and in accordance with the results obtained from U937 cells (Supplementary Fig. 3–9). We showed that overexpression of S100A8 in AML cells can trigger ROS generation via NOX2 activation, thereby promoting senescence of BMSCs. Aging BMSCs can secrete a variety of cytokines that exert stimulatory effects on the progression of AML. (Fig. 6). Besides, we also demonstrated that co-culture with HS-5 cells could inhibit the sensitivity of U937 to chemotherapy drugs (Ara-C + DNR) (Supplementary Fig. 10). The present study reveals the crucial involvement of the S100A8-NOX2-ROS signaling pathway in mediating the communication between AML cells and BMSCs. It is essential to recognize that there are still some limitations in this study. We initially established a co-culture system comprising the AML cell line U937 and stromal cell HS-5, subsequently validating the experimental findings in another AML cell line HL-60, thereby substantiating the generalizability of our conclusions. The HL-60 cell line is derived from promyelocytes, while the U937 cell line represents acute mononuclear leukemia cells, thus representing two distinct subtypes of acute myeloid leukemia. Since AML is highly heterogeneous, we should further validate our findings in other types of AML cells, as well as in primary leukemia cells and in animal models of AML, to demonstrate the generalizability of our conclusions. We will continue our research in the future.

In addition, several proteins were identified by proteomic analysis that may have a potential as therapeutic targets or markers for AML (Supplementary Table S2). ANXA2 was upregulated after co-culture and is a member of the annexin phospholipid-binding protein family[36]. In ovarian cancer xenograft mice, the administration of CAR (2448)-T cells targeting ANXA2 resulted in tumor eradication and prolonged survival[37].Additionally, the sequential administration of Lm-ANXA2, a Listeria monocytogenes vaccine against ANXA2, along with anti-PD-1 antibody, induced modifications in the pancreatic cancer microenvironment. This resulted in enhanced specific T-cell responses within the tumor microenvironment and further prolonged survival in murine models[38]. High level of *ANXA2* mRNA was associated with poor prognosis in adult AML[39]. The potential of ANXA2 as a promising candidate for AML immunotherapy or combination therapy requires further investigation. Proteomic analysis in this study revealed high ASPH expression after co-culturing with HS-5 cells. ASPH is a tumor-associated antigen (TAA) that is expressed at the cell surface, creating a possibility for it to be a potential target for immunotherapy in malignancies including hepatocellular carcinoma (HCC), triple-negative breast cancer (TNBC) and others[40–42]. ASPH is significantly upregulated in around 40% of AML patients[43]. The application of anti-ASPH radiolabeled or cytotoxin-conjugated antibody–drug conjugates (ADCs) was effective in killing AML cell line MOLM-14 in vitro[44], providing preliminary evidence for ASPH as a potential target for immunotherapy in the treatment of AML. The resultant changes in proteomic analysis may furnish novel therapeutic targets or markers for AML.

U937 and HL-60 cells co-cultured with HS-5 cells exhibited a significant upregulation in NOX2 activity and increased production of extracellular levels of ROS. The high expression of NOX2 in leukemia cells and the elevated levels of extracellular ROS have been observed in more than 60% of primary AML patients, which is

associated with an unfavorable prognosis[15]. ROS are important second messengers in normal hematopoiesis. The role of ROS in AML development is dual-fold. They induce the molecular genetic changes that promote tumor initiation and progression[45]. Meanwhile, they can exert cytotoxic effects on AML cells through oxidative stress-dependent mechanisms, including apoptosis and autophagic cell death[46,47]. NOX2 and mitochondria are the two main sources of cellular ROS. Elevated levels of ROS are commonly observed in AML cells[48,49]. However, the intracellular ROS levels decreased in HL-60 and U937 cells co-cultured with HS-5 cells. The presence of a robust antioxidant system within AML cells may contribute to the mitigation of elevated ROS[50–52], which is associated with BMSCs[52]. Previous studies showed that the enzyme SOD2 plays a crucial role in mitigating the excessive production of ROS by mitochondria[53,54], converting them into harmless H_2O_2 and O_2 through enzymatic reactions[55]. Proteomic analysis revealed a significant up-regulation of SOD2 (Supplementary Table S2), which may be attributed to a decrease rather than an increase in intracellular ROS levels. The intricate regulation of the antioxidant system in leukemia cells remains a subject of controversy[56,57]. In this study co-culture system, we found that HS-5 cells induced an increase in NOX2 enzyme activity in AML cells, resulting in the production of extracellular ROS. Additionally, HS-5 cells might alter the antioxidant system of AML cells, enabling them to withstand prolonged oxidative stress without surpassing the lethal threshold, thereby maintaining low levels of intracellular ROS. Further research is required into the ways in which BMSCs influences intra- and extracellular ROS homeostasis in AML cells, as well as the impact on the antioxidant system.

During AML development, leukemia cells cause remodeling of the BMM[7], which in turn significantly impacts the support of normal hematopoiesis by BMSCs, leading to hematopoietic insufficiency[58]. The senescence indices of BMSCs derived from AML patients were shown to be significantly higher compared to those of healthy donors within the same age group[59]. In the present study, HS-5 cells exhibited a senescence phenotype after co-culture with AML cells, characterized by elevated levels of SA-β-Gal and up-regulated mRNA expression of IL-6, IL-8 and others[27,60] (Fig. 4). Knockdown of S100A8 in AML cells resulted in the reversal of the senescence phenotype observed in HS-5 cells. This suggests that targeting S100A8 in AML cells may have the potential to reverse the senescence phenotype of BMSCs, which may represent a promising therapeutic strategy to improve the AML microenvironment and treat AML. As cytokines may create a pro-inflammatory environment, and mediate the progression of AML[61]. Aging BMSCs can produce a variety of SASP and release them into the microenvironment[15]. Thus, we examined cytokine levels in the supernatants of HL-60 and U937 cells co-cultured with or without HS-5 cells, and in HS-5 cells alone using a cytokine array. The analysis revealed an elevation of the levels of cytokines, including IL-6, CXCL5, and Angiogenin in the supernatants of the co-culture system (Fig. 5, Supplementary Fig. 8–9). It has been reported that IL-6 can enhance S100A8 expression in AML cells via the JAK-STAT3 signaling pathway[62], thereby potentially initiating a feedback loop that modulates the BMSCs. CXCL5 plays a pivotal role in the CXCLs/CXCR crosstalk network within the microenvironment[63], and is implicated in the migration of CD34-/low LSC from the BM to the vascular ecotone for release into the periphery[64]. Consequently, targeting the CXCL5/CXCR2 signaling pathway has the potential to enhance the effects of TKIs on FLT3-AML[65]. The microvessel count is elevated in the bone marrow of patients with AML[66]. Brunner B. et al. found that Angiogenin was up-regulated in patients with bone marrow malignancies [67]. Angiogenin is a potent inducer of angiogenesis that mediates bone marrow angiogenesis in leukemia[68–70]. We observed that following the downregulation of S100A8 in AML cells, a significant reduction in the cytokine levels of IL-6, CXCL5 and Angiopoietin was found in the co-culture supernatant (Fig. 5, Supplementary Fig. 8–9). These further indicate that S100A8 may affect the cytokine network in the leukemia microenvironment.

In summary, we provide preliminary evidence that S100A8 may be a key regulator in the communication between AML cells and BMSCs. The overexpression of S100A8 in AML cells can induce ROS generation via NOX2 activation and promote senescence in BMSCs, concurrently influencing the cytokine composition of the microenvironment. Cytokines secreted by aging BMSCs exert stimulatory effects on the progression of AML. Specific inhibitors targeting S100A8 are already in existence, and targeting S100A8 is likely to be an effective strategy for the treatment of AML.

Materials & methods

Cell lines and culture conditions

Cells were cultured at 37 ℃ in a humidified incubator set to 5% CO_2. Human AML cell lines (U937 and HL-60), purchased from the Cell Bank of Type Culture Collection of the Chinese Academy of Sciences (Shanghai, China), were maintained in RPMI-1640 medium (Sigma-Aldrich, St. Louis, MO), supplemented with 10% fetal bovine serum (FBS, Cegrogen Biotech, Germany). HS-5, a type of human bone marrow stromal cells, were purchased from the American Type Culture Collection (ATCC, Manassas, VA, USA) and cultured in Dulbecco's Modified Eagle's Medium (DMEM/High, Sigma-Aldrich) supplemented with 10% FBS.

AML cells and HS-5 co-culture system

HS-5 cells were seeded at 1×10^5 cells in 6-well plates and cultured for 24 h. until they reach approximately 80% confluence. They were then co-cultured for 48 h. with 2×10^5 AML cells (U937 or HL-60) for the establishment of the in vitro co-culture system. Most AML cells were then collected by gently pipetting twice with 1X cold PBS, followed by PBS/EDTA. As AML cells express CD45, they were purified for subsequent experiments using a human CD45 positive selection kit (STEMCELL Technologies, Vancouver, BC). coc means co-culture; moc is the abbreviation of mono-cluture.

Cell viability assay

Cell viability was evaluated with the MTS assay kit (Promega Corporation, Madison, WI, USA). U937 co-cultured with or without HS-5 were seeded in 96-well plates at a density of 10,000 cells per well, while HL-60 were seeded at a density of 20,000 cells per well. The cell culture medium (200 μl) was used as control and

incubated along the cells at 37 ℃ with 5% CO_2 in a humidified atmosphere for 24 h. MTS (40 µl) was added to each well and the absorbance of each well was detected at a 490/630 nm dual wavelength with a microplate reader (ThermoFisher Scientific).

Apoptosis analysis

AML cells co-cultured with or without HS-5 were harvested by pipetting, rinsed three times with 1X cold PBS, resuspended in 100 µl 1X binding buffer, and then stained with 5 µl Annexin V-FITC and 5 µl PI for 15 min. at room temperature in the dark. Samples were then diluted with 400 µl 1X binding buffer before FACS analysis using a flow cytometer (Accuri C6 Plus, BD Biosciences, San Jose, CA, USA). Results were analyzed using the FlowJo 10.1 software.

Protein extraction and analysis by LC–MS/MS

U937 and HL-60 co-cultured with or without HS-5 were collected, washed with 1X PBS three times, centrifuged, and the recovered cell pellet was frozen in liquid nitrogen and stored at -80℃. Samples, including three replicates per test group, were sent to Shanghai Zhongke New Life Company for proteomics analysis. Raw data were analyzed for identification and quantitative analysis using the MaxQuant software (version 1.6.14). The label-free quantification (LFQ) intensity of proteins was determined by averaging the three replicates and used to calculate the fold change values (Fc). Proteins were considered up-regulated when Fc was > 2 and $p < 0.05$ and down-regulated when Fc was < 0.5 and $p < 0.05$.

Bioinformatics analysis

KEGG enrichment analysis was performed on the differentially expressed proteins. Fisher's Exact Test (FET) was used to compare the distribution of individual KEGG pathways for the differentially expressed proteins and total proteins. The Wayne plot, protein heatmap and KEGG enriched bubble plot were obtained using the OmicStudio tools (https://www.omicstudio.cn/tool).

Real-time quantitative PCR (RT-qPCR)

Total RNA was extracted using the RNA-Easy isolation reagent (Vazyme Biotech, Nanjing, China). cDNA was synthesized using the Hifair III 1st Strand cDNA Synthesis SuperMix for qPCR (Yeasen Biotech, Shanghai, China), while real-time PCR was performed using the Hieff qPCR SYBR Green Master Mix (Yeasen Biotech, Shanghai, China). Primer sequences are provided in the Supplementary Table S1. GAPDH was used as the internal control, and the $2^{-\Delta\Delta CT}$ method was used to analyze the expression levels of genes.

Western blot analysis

Protein lysates were extracted using the RIPA lysis buffer (Vazyme Biotech, Nanjing, China) containing a protease and phosphatase inhibitor cocktail (#PPC1010, Sigma-Aldrich, St. Louis, MO, USA). Lysates were separated by 12% SDS-PAGE. The antibody against S100A8 was from Abcam (Cambridge, MA, USA), while that against NOX2 was from Immunoway (Beijing, China) and that against GAPDH was from Immunoway (Suzhou, China). Quantification of the protein bands was performed by densitometry and analyzed using the Image J 1.43 software.

Lentiviral transduction for S100A8 knockdown

Short hairpin RNA (shRNA) was purchased from Gene Pharma Company (Shanghai, China). The shRNA targeting the S100A8 gene had the antisense:

5′-TCAACACTGATGGTGCAGTTA-3′,
5′-GTGTCCTCAGTATATCAGGAA-3′,
5′-CCUGAAGAAAUUGCUAGAGTT-3′.

Two groups were established, the knockdown group (KD group, transfected with S100A8-shRNA-LV) and the negative group (NC group, transfected with scramble-shRNA-LV). Transfected cells were then grown in medium containing 1 µg/ml puromycin for selection.

Detection of Intracellular ROS

AML cells cultured under different conditions were washed twice with 1X PBS. DCFH-DA (2',7'-Dichlorodihydrofluorescein diacetate), a cell-permeable probe, was used to detect intracellular ROS. AML cells were incubated with 10 µM DCFH-DA (Beyotime Institute of Biotechnology, Hangzhou, China) for 20 min at 37 °C; cells were then washed three times with 1X PBS and resuspended in RPMI-1640 medium for FACS analysis.

Amplex red assay

Peroxidase levels in AML cells with different treatments, as well as peroxide levels in the supernatants, were assessed by using the Amplex™ red hydrogen peroxide/peroxidase analysis kit (Thermo Fisher Scientific, Waltham, MA, USA). A total of 15,000 cells resuspended in Krebs–Ringer Phosphate buffer (Solarbio, Beijing, China) or 50 µl of supernatant were added to a 96-well plate to detect NADPH oxidase activity or superoxide production, and analyses were carried out according to the manufacturer's protocol.

Senescence-associated β-Galactosidase (SA-β-Gal) staining

Cell senescence was evaluated using the SA-β-gal staining kit (Beyotime, Shanghai, China). Briefly, the cells were washed with 1X PBS and incubated in the fixation solution for 15 min. at room temperature. Afterwards, the cells were washed with 1X PBS and incubated overnight in the SA-β-Gal staining solution at 37 °C. The images

were captured using an inverted microscope (Olympus, Tokyo, Japan), and the percentage of SA-β-Gal-positive cells was determined and results were obtained from three independent experimental replicates.

EdU staining

Cell proliferation was assessed using an EdU Cell Proliferation Kit with Alexa Fluor 488 kit (Epizyme, Shanghai, China). The cell nuclei were co-stained with DAPI (Solarbio, Beijing, China) for 10 min. and counted using a fluorescence microscope (Olympus, Tokyo, Japan).

Cytokine array

The cell supernatants were collected and centrifuged at 800x*g* for 10 min. to remove floating cells and debris. An unbiased human cytokine screening was carried out using the ELISA-based 80-target cytokine array kit (Abcam, Cambridge, MA, USA). The 11 × 8 format comprised 14 interleukins (ILs, brown), 27 chemokines (CKs, blue) and 39 other cytokines (yellow, including growth factors, colony-stimulating factors, receptors, etc.). Please see Fig. 6A.

Statistical analyses

All quantitative variables were presented as mean ± standard deviation. All statistical analyses were performed using the SPSS statistical software version 26.0. Two group comparisons were performed using a two-tailed Student's t-test. Additionally, one-way ANOVA with a least significant difference post hoc test was used to compare mean values between multiple groups, and a two-tailed, two-way ANOVA was utilized in multiple comparisons, followed by the Bonferroni post hoc analysis to identify interactions. Results were considered significant when $p < 0.05$.

Data availability

All data generated or analyzed during this study are included in this article and its supplementary information files.If anyone would like data from this study, please contact corresponding author Professor Jianping Xu（jianpingxu@fjmu.edu.cn）.

Received: 17 December 2024; Accepted: 7 May 2025
Published online: 17 May 2025

References

1. Döhner, H., Weisdorf, D. J. & Bloomfield, C. D. Acute myeloid Leukemia. *N. Engl. J. Med.* **373**(12), 1136–1152 (2015).
2. De Kouchkovsky, I. & Abdul-Hay, M. Acute myeloid leukemia: a comprehensive review and 2016 update. *Blood Cancer J.* **6**(7), e441 (2016).
3. Krause, D. S. & Scadden, D. T. A hostel for the hostile: the bone marrow niche in hematologic neoplasms. *Haematologica* **100**(11), 1376–1387 (2015).
4. Sendker, S., Waack, K. & Reinhardt, D. Far from health: the bone marrow microenvironment in aml, a leukemia supportive shelter. *Children (Basel).* **8**(5), 371 (2021).
5. Battula, V. L. et al. Acute myeloid leukemia cells acquire stem cell features in the bone marrow microenvironment. *Clin. Lymphoma Myeloma Leuk.* **14**, S119–S120 (2014).
6. Joshi, S. K. et al. The AML microenvironment catalyzes a stepwise evolution to gilteritinib resistance. *Cancer Cell* **39**(7), 999-1014. e1018 (2021).
7. Ennis, S. et al. Cell-cell interactome of the hematopoietic niche and its changes in acute myeloid leukemia. *iScience.* **26**(6), 106943 (2023).
8. Battula, V. L. et al. AML-induced osteogenic differentiation in mesenchymal stromal cells supports leukemia growth. *JCI Insight.* **2**(13), e90036 (2017).
9. Heizmann, C. W. & Cox, J. A. New perspectives on S100 proteins: a multi-functional Ca(2+)-, Zn(2+)- and Cu(2+)-binding protein family. *Biometals* **11**(4), 383–397 (1998).
10. Chen, Y., Ouyang, Y., Li, Z., Wang, X. & Ma, J. S100A8 and S100A9 in Cancer. *Biochim. Biophys. Acta. Rev. Cancer.* **1878**(3), 188891 (2023).
11. Bresnick, A. R., Weber, D. J. & Zimmer, D. B. S100 proteins in cancer. *Nat. Rev. Cancer.* **15**(2), 96–109 (2015).
12. Nicolas, E. et al. Expression of S100A8 in leukemic cells predicts poor survival in de novo AML patients. *Leukemia* **25**(1), 57–65 (2011).
13. Laouedj, M. et al. S100A9 induces differentiation of acute myeloid leukemia cells through TLR4. *Blood* **129**(14), 1980–1990 (2017).
14. Bedard, K. & Krause, K. H. The NOX family of ROS-generating NADPH oxidases: physiology and pathophysiology. *Physiol. Rev.* **87**(1), 245–313 (2007).
15. Hole, P. S. et al. Overproduction of NOX-derived ROS in AML promotes proliferation and is associated with defective oxidative stress signaling. *Blood* **122**(19), 3322–3330 (2013).
16. Robinson, A. J. et al. Reactive oxygen species drive proliferation in acute myeloid leukemia via the glycolytic regulator PFKFB3. *Cancer Res.* **80**(5), 937–949 (2020).
17. Marlein, C. R. et al. NADPH oxidase-2 derived superoxide drives mitochondrial transfer from bone marrow stromal cells to leukemic blasts. *Blood* **130**(14), 1649–1660 (2017).
18. Kerkhoff, C. et al. The arachidonic acid-binding protein S100A8/A9 promotes NADPH oxidase activation by interaction with p67phox and Rac-2. *Faseb. J.* **19**(3), 467–469 (2005).
19. Tao, Q. et al. S100A8 regulates autophagy-dependent ferroptosis in microglia after experimental subarachnoid hemorrhage. *Exp. Neurol.* **357**, 114171 (2022).
20. Weinberg, F., Ramnath, N. & Nagrath, D. Reactive oxygen species in the tumor microenvironment: an overview. *Cancers (Basel).* **11**(8), 1191 (2019).
21. Chatterjee, R. & Law, S. Epigenetic and microenvironmental alterations in bone marrow associated with ROS in experimental aplastic anemia. *Eur. J. Cell Biol.* **97**(1), 32–43 (2018).
22. Plakhova, N., Panagopoulos, V., Vandyke, K., Zannettino, A. C. W. & Mrozik, K. M. Mesenchymal stromal cell senescence in haematological malignancies. *Cancer Metastasis Rev.* **42**(1), 277–296 (2023).
23. Hu, D. et al. Cellular senescence and hematological malignancies: From pathogenesis to therapeutics. *Pharmacol. Ther.* **223**, 107817 (2021).

24. Kim, Y. et al. Genetic and epigenetic alterations of bone marrow stromal cells in myelodysplastic syndrome and acute myeloid leukemia patients. *Stem Cell Res.* **14**(2), 177–184 (2015).
25. Vanegas, N. P., Ruiz-Aparicio, P. F., Uribe, G. I., Linares-Ballesteros, A. & Vernot, J. P. Leukemia-induced cellular senescence and stemness alterations in mesenchymal stem cells are reversible upon withdrawal of B-cell acute lymphoblastic Leukemia cells. *Int. J. Mol. Sci.* **22**(15), 8166 (2021).
26. Abdul-Aziz, A. M. et al. Acute myeloid leukemia induces protumoral p16INK4a-driven senescence in the bone marrow microenvironment. *Blood* **133**(5), 446–456 (2019).
27. Gorgoulis, V. et al. Cellular senescence: defining a path forward. *Cell* **179**(4), 813–827 (2019).
28. Cheng, J. et al. CXCL8 derived from mesenchymal stromal cells supports survival and proliferation of acute myeloid leukemia cells through the PI3K/AKT pathway. *Faseb. J.* **33**(4), 4755–4764 (2019).
29. Habbel, J. et al. Inflammation-driven activation of JAK/STAT signaling reversibly accelerates acute myeloid leukemia in vitro. *Blood Adv.* **4**(13), 3000–3010 (2020).
30. Leimkühler, N. B. & Schneider, R. K. Inflammatory bone marrow microenvironment. *Hematol. Am. Soc. Hematol. Educ. Program.* **2019**(1), 294–302 (2019).
31. Çelik, H. et al. Highly multiplexed proteomic assessment of human bone marrow in acute myeloid leukemia. *Blood Adv.* **4**(2), 367–379 (2020).
32. Sun, Y. X. et al. The imbalanced profile and clinical significance of T helper associated cytokines in bone marrow microenvironment of the patients with acute myeloid leukemia. *Hum. Immunol.* **75**(2), 113–118 (2014).
33. Van Etten, R. A. Aberrant cytokine signaling in leukemia. *Oncogene* **26**(47), 6738–6749 (2007).
34. Karimdadi Sariani, O., Eghbalpour, S., Kazemi, E., Rafiei Buzhani, K. & Zaker, F. Pathogenic and therapeutic roles of cytokines in acute myeloid leukemia. *Cytokine* **142**, 155508 (2021).
35. Azadniv, M. et al. Bone marrow mesenchymal stromal cells from acute myelogenous leukemia patients demonstrate adipogenic differentiation propensity with implications for leukemia cell support. *Leukemia* **34**(2), 391–403 (2020).
36. Grieve, A. G., Moss, S. E. & Hayes, M. J. Annexin A2 at the interface of actin and membrane dynamics: a focus on its roles in endocytosis and cell polarization. *Int. J. Cell Biol.* **2012**, 852430 (2012).
37. Leong, L. et al. Preclinical activity of embryonic annexin A2-specific chimeric antigen receptor T cells against ovarian cancer. *Int. J. Mol. Sci.* **21**(2), 381 (2020).
38. Kim, V. M. et al. Anti-pancreatic tumor efficacy of a Listeria-based, Annexin A2-targeting immunotherapy in combination with anti-PD-1 antibodies. *J. Immunother. Cancer.* **7**(1), 132 (2019).
39. Niu, Y. et al. Distinct prognostic values of Annexin family members expression in acute myeloid leukemia. *Clin. Transl. Oncol.* **21**(9), 1186–1196 (2019).
40. Linja, M. J. et al. Amplification and overexpression of androgen receptor gene in hormone-refractory prostate cancer. *Cancer Res.* **61**(9), 3550–3555 (2001).
41. Aihara, A. et al. A cell-surface β-hydroxylase is a biomarker and therapeutic target for hepatocellular carcinoma. *Hepatology* **60**(4), 1302–1313 (2014).
42. Bai, X. et al. Adaptive antitumor immune response stimulated by bio-nanoparticle based vaccine and checkpoint blockade. *J. Exp. Clin Cancer Res.* **41**(1), 132 (2022).
43. Holtzman, N. G. et al. Aspartate β-hydroxylase (ASPH) expression in acute myeloid leukemia: a potential novel therapeutic target. *Front. Oncol.* **11**, 783–744 (2021).
44. Lebowitz, M. S. et al. Radioimmunotherapy for acute myeloid leukemia targeting human aspartyl (asparaginyl) β-hydroxylase. *Blood* **77**, 2650–2650 (2017).
45. Sallmyr, A., Fan, J. & Rassool, F. V. Genomic instability in myeloid malignancies: increased reactive oxygen species (ROS), DNA double strand breaks (DSBs) and error-prone repair. *Cancer Lett.* **270**(1), 1–9 (2008).
46. Yang, Y. et al. Camalexin induces apoptosis via the ROS-ER Stress-mitochondrial apoptosis pathway in AML cells. *Oxid. Med. Cell Longev.* **2018**, 7426950 (2018).
47. Xiong, X. X. et al. Piperlongumine induces apoptotic and autophagic death of the primary myeloid leukemia cells from patients via activation of ROS-p38/JNK pathways. *Acta. Pharmacol. Sin.* **36**(3), 362–374 (2015).
48. Li, L. et al. Altered hematopoietic cell gene expression precedes development of therapy-related myelodysplasia/acute myeloid leukemia and identifies patients at risk. *Cancer Cell* **20**(5), 591–605 (2011).
49. Er, T. K. et al. Antioxidant status and superoxide anion radical generation in acute myeloid leukemia. *Clin. Biochem.* **40**(13–14), 1015–1019 (2007).
50. Forte, D. et al. Bone marrow mesenchymal stem cells support acute myeloid Leukemia bioenergetics and enhance antioxidant defense and escape from chemotherapy. *Cell Metab.* **32**(5), 829-843.e829 (2020).
51. Abdul-Aziz, A., MacEwan, D. J., Bowles, K. M. & Rushworth, S. A. Oxidative stress responses and NRF2 in human leukaemia. *Oxid. Med. Cell Longev.* **2015**, 454659 (2015).
52. Trombetti, S. et al. Oxidative stress and ROS-mediated signaling in Leukemia: novel promising perspectives to eradicate chemoresistant cells in myeloid Leukemia. *Int. J. Mol. Sci.* **22**(5), 2470 (2021).
53. Zou, X. et al. Manganese superoxide dismutase (SOD2): is there a center in the universe of mitochondrial redox signaling?. *J. Bioenerg. Biomembr.* **49**(4), 325–333 (2017).
54. Chen, C. et al. Mitochondria and oxidative stress in ovarian endometriosis. *Free Radic. Biol. Med.* **136**, 22–34 (2019).
55. Culotta, V. C. Superoxide dismutase, oxidative stress, and cell metabolism. *Curr. Top Cell Regul.* **36**, 117–132 (2000).
56. Zhou, F. et al. Jab1/Csn5-thioredoxin signaling in relapsed acute monocytic leukemia under oxidative stress. *Clin. Cancer Res.* **23**(15), 4450–4461 (2017).
57. Irwin, M. E., Rivera-Del Valle, N. & Chandra, J. Redox control of leukemia: from molecular mechanisms to therapeutic opportunities. *Antioxid. Redox. Signal.* **18**(11), 1349–1383 (2013).
58. Hanoun, M. et al. Acute myelogenous leukemia-induced sympathetic neuropathy promotes malignancy in an altered hematopoietic stem cell niche. *Cell Stem Cell* **15**(3), 365–375 (2014).
59. Kornblau, S. M. et al. Distinct protein signatures of acute myeloid leukemia bone marrow-derived stromal cells are prognostic for patient survival. *Haematologica* **103**(5), 810–821 (2018).
60. Tsirpanlis, G. Cellular senescence and inflammation: a noteworthy link. *Blood Purif.* **28**(1), 12–14 (2009).
61. Hemmati, S., Haque, T. & Gritsman, K. Inflammatory signaling pathways in preleukemic and leukemic stem cells. *Front. Oncol.* **7**, 265 (2017).
62. Böttcher, M. et al. Bone marrow stroma cells promote induction of a chemoresistant and prognostic unfavorable S100A8/A9high AML cell subset. *Blood Adv.* **6**(21), 5685–5697 (2022).
63. Kittang, A. O. et al. The chemokine network in acute myelogenous leukemia: molecular mechanisms involved in leukemogenesis and therapeutic implications. *Curr. Top Microbiol. Immunol.* **341**, 149–172 (2010).
64. Yoon, K. A. et al. Differential regulation of CXCL5 by FGF2 in osteoblastic and endothelial niche cells supports hematopoietic stem cell migration. *Stem Cells Dev.* **21**(18), 3391–3402 (2012).
65. Cao, H. et al. Targeting TKI-activated NFKB2-MIF/CXCLs-CXCR2 signaling pathways in FLT3 mutated acute myeloid leukemia reduced blast viability. *Biomedicines.* **10**(5), 1038 (2022).
66. Padró, T. et al. Increased angiogenesis in the bone marrow of patients with acute myeloid leukemia. *Blood* **95**(8), 2637–2644 (2000).

67. Brunner, B. et al. Blood levels of angiogenin and vascular endothelial growth factor are elevated in myelodysplastic syndromes and in acute myeloid leukemia. *J. Hematother. Stem Cell Res.* **11**(1), 119–125 (2002).
68. Vliora, M. et al. The impact of adipokines on vascular networks in adipose tissue. *Cytokine Growth Factor Rev.* **69**, 61–72 (2023).
69. Wakabayashi, M. et al. Autocrine pathway of angiopoietins-Tie2 system in AML cells: association with phosphatidyl-inositol 3 kinase. *Hematol. J.* **5**(4), 353–360 (2004).
70. Maffei, R. et al. Increased angiogenesis induced by chronic lymphocytic leukemia B cells is mediated by leukemia-derived Ang2 and VEGF. *Leuk Res.* **34**(3), 312–321 (2010).

Author contributions
All authors have read and agreed to the published version of the manuscript. Jianping Xu, Guanbin Zhang : Conceptualization, methodology, formal analysis ; Yangyang Gu, Jingyi Xia, Yuhong Guo: investigation ; Linfen Tao: data analysis; Yangyang Gu, Jingyi Xia: writing—original draft preparation, writing—review and editing .

Funding
Supported by Science Foundation of the Fujian Province (grant no. 2021J01814).

Declarations

Competing interests
The authors declare no competing interests.

Additional information
Supplementary Information The online version contains supplementary material available at https://doi.org/10.1038/s41598-025-01711-x.

Correspondence and requests for materials should be addressed to G.Z. or J.X.